JTTEE5 14:315-320
DOI: 10.1361/105996305X59396
1059-9630/$19.00 © ASM International

Characterization of Oxide Scales Formed on High-Velocity Oxyfuel-Sprayed Ni-Co-Cr-Al-Y + ReTa Coatings

D.B. Lee, J.H. Ko, and J.H. Yi

(Submitted February 13, 2004; in revised form June 8, 2004)

A high-velocity oxyfuel-sprayed 30 wt.% Ni-20 wt.% Co-30 wt.% Cr-10 wt.% Al-2 wt.% Y-4 wt.% Re-4 wt.% Ta coating was oxidized between 1000 and 1200 °C for up to 200 h in air, and the oxide scales were examined. The dense, sprayed coating consisted mainly of Cr_3Ni_2, Ni_3Al, Ni_3Ta, Ni, NiO, $Al_5Y_3O_{12}$, and Cr_2O_3. Intermetallics and some oxides formed during spraying. During oxidation, mainly αAl_2O_3, along with some $Al_5Y_3O_{12}$, $CoAl_2O_4$, $CoCr_2O_4$, Ta_2O_5, and $Ta_2O_{2.2}$ formed on the coating. The preferential oxidation of Al to form the Al-rich scales resulted in the formation of an Al-depleted region beneath the scales. Rhenium, being the most noble element, was distributed throughout the oxide scale and the coating, without forming any independent oxides.

Keywords coating, Ni-Co-Cr-Al-Y, oxidation, rhenium, tantalum

1. Introduction

Duplex thermal barrier coatings (TBCs) that consist of a thermally insulating ceramic top coating and an oxidation-resistant metallic bond coating are used to protect the hot-section components of gas turbines against oxidation, corrosion, and erosion in service. Zirconia, which is partially stabilized by various oxides (PSZ), is commonly applied to the plasma-sprayed MCrAlY bond coating (M = Ni, Co). Much effort has been made to develop advanced coatings for the purpose of designing more efficient engines with greater fuel economy and lower electrical energy cost (Ref 1, 2). For this purpose, Ni-Co-Cr-Al-Y coatings have been developed, with or without Re or Ta, and their oxidation behavior has previously been studied.

The oxidation of Ni-Co-Cr-Al-Y + Re coatings between 850 and 1200 °C in air has been extensively studied (Ref 3-9). The addition of 1 to 10 wt.% Re considerably improved the oxidation and thermomechanical fatigue properties (Ref 6-8, 10). However, the high-temperature oxidation of Ni-Co-Cr-Al-Y + Ta coatings has scarcely been studied. According to Frances et al. (Ref 11), the oxidation of low-pressure plasma-sprayed (LPPS) Ni-Co-Cr-Al-Y + 3.5 to 4.5 wt.% Ta coatings (Amdry 997; Sulzer Metco, Westbury, NY) at 850 °C in air resulted in the growth of a homogeneous and compact Al_2O_3 layer, with limited scale spallation. However, as far as we know, the oxidation of Ni-Co-Cr-Al-Y coatings containing both Re and Ta has not been reported.

In this study, gas-atomized Ni-Co-Cr-Al-Y + ReTa alloy powders were sprayed onto a Ni-based substrate using the high-velocity oxyfuel (HVOF) process. They were then oxidized at high temperatures, and the oxide scales that formed were investigated. The purpose of this study was to clarify the oxidation products and to discuss the results obtained in comparison with those of previous studies of Ni-Co-Cr-Al-Y + (Ta or Re) bond coatings.

D.B. Lee and **J.H. Ko,** Department of Advanced Materials Engineering, Sungkyunkwan University, Suwon 440-746, South Korea; and **J.H. Yi,** Gas Turbine Service Center, Korea Plant Service & Engineering, Inchon 440-170, South Korea. Contact e-mail: dlee@yurim.skku.ac.kr.

2. Experimental Procedure

Gas-atomized 30 wt.% Ni-20 wt.% Co-30 wt.% Cr-10 wt.% Al-2 wt.% Y-4 wt.% Re-4 wt.% Ta (hereafter, referred to as Ni-Co-Cr-Al-Y + ReTa) with a particle size of −62 + 11 μm was HVOF-sprayed onto a Hastelloy-X (Haynes, Int., Kokomo, IN) (49.0 wt.% Ni-22.0 wt.% Cr-15.8 wt.% Fe-9.0 wt.% Mo-1.5 wt.% Co-2.0 wt.% Al-0.6 wt.% W-0.15 wt.% C) plate using a Sulzer Metco DJ 2600 system. The compositions indicated in this study are all in weight percent, unless otherwise stated. Before spraying, the substrate was grit-blasted with grade 60 alumina powders. The detailed spraying parameters are listed in Table 1. The coating was about 250 μm thick.

After being cut into samples with a size of 10 × 10 × 15 mm^3, separate samples of the prepared Ni-Co-Cr-Al-Y + ReTa coating were oxidized isothermally in a muffle furnace in atmospheric air for up to 200 h at temperatures of 1000, 1100, and 1200 °C, respectively. The specimens before and after oxidation were inspected by x-ray diffraction (XRD), a scanning electron microscope (SEM), and an electron probe microanalyzer (EPMA).

Table 1 HVOF deposition condition

Parameters	Settings
Spray distance	300 mm
Transverse speed	750 mm/s
Fuel gas type	H_2
Fuel gas flow	1600 ft^2/h
Oxygen gas flow	380 ft^2/h
Air cap flow	800 ft^2/h
Carrier gas flow	29 ft^2/h

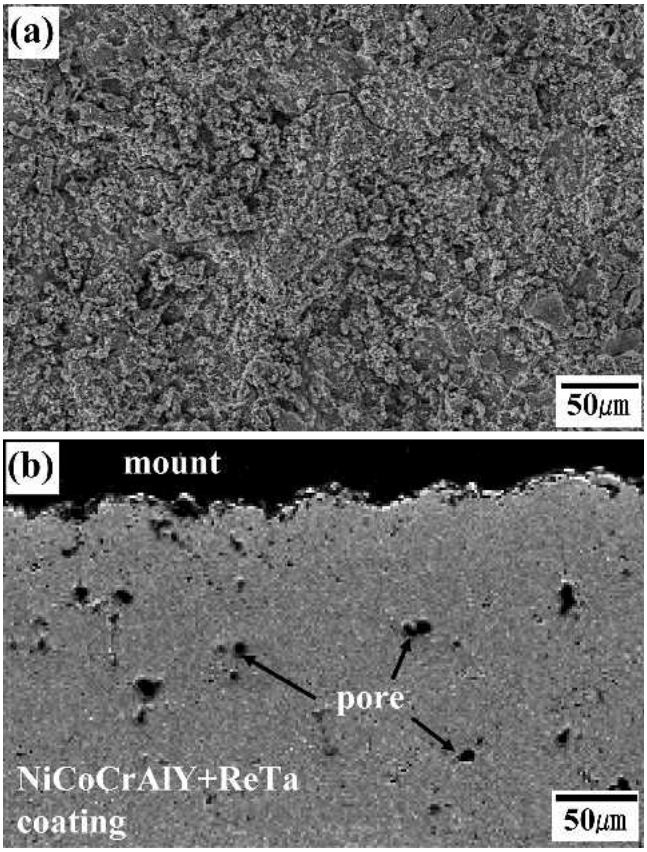

Fig. 1 SEM image of as-sprayed Ni-Co-Cr-Al-Y + ReTa coating: (a) top view and (b) cross section

3. Results and Discussion

Figure 1 shows the SEM top view and the cross-sectional image of the as-sprayed Ni-Co-Cr-Al-Y + ReTa coating. The coating surface shown in Fig. 1(a) displays a relatively rough surface due to the molten splat strike layer by layer and the turbulent cooling jet during spraying. Because splats strike the surface with considerable supersonic force, flattened splats have a low level of internal pores, as shown in Fig. 1(b). It is noted that the amount of internal oxide stringers, cracks, and pores can be considerably reduced by adopting the HVOF process, rather than the air plasma spray coating technique (Ref 12). Oxygen from the atmosphere penetrates into the coating via cracks and open pores, which results in internal oxidation causing the harmful preconsumption of Al and poor scale adhesion (Ref 12, 13). On the other hand, pores also have the beneficial effect of improving the thermal shock resistance and thermal barrier efficiency.

Figure 2 shows the XRD patterns of the Ni-Co-Cr-Al-Y + ReTa coating before and after the high-temperature oxidation. The XRD pattern of the as-sprayed coating shown in Fig. 2(a) indicates that the prepared coating consists primarily of Cr_3Ni_2, Ni_3Al, Ni_3Ta, Ni, NiO, $Al_5Y_3O_{12}$, and Cr_2O_3, in order of decreasing content. The yttrium present in the coating was highly susceptible to oxidation during the HVOF spraying process, due to its high oxygen affinity (Ref 5). The XRD patterns after oxidation are shown in Fig. 2(b) to (d). Because the scales were thin, some unoxidized coating peaks, such as those corresponding to Cr_3Ni_2, Ni_3Al, Ni_3Ta, and Ni, were seen. As the oxidation pro-

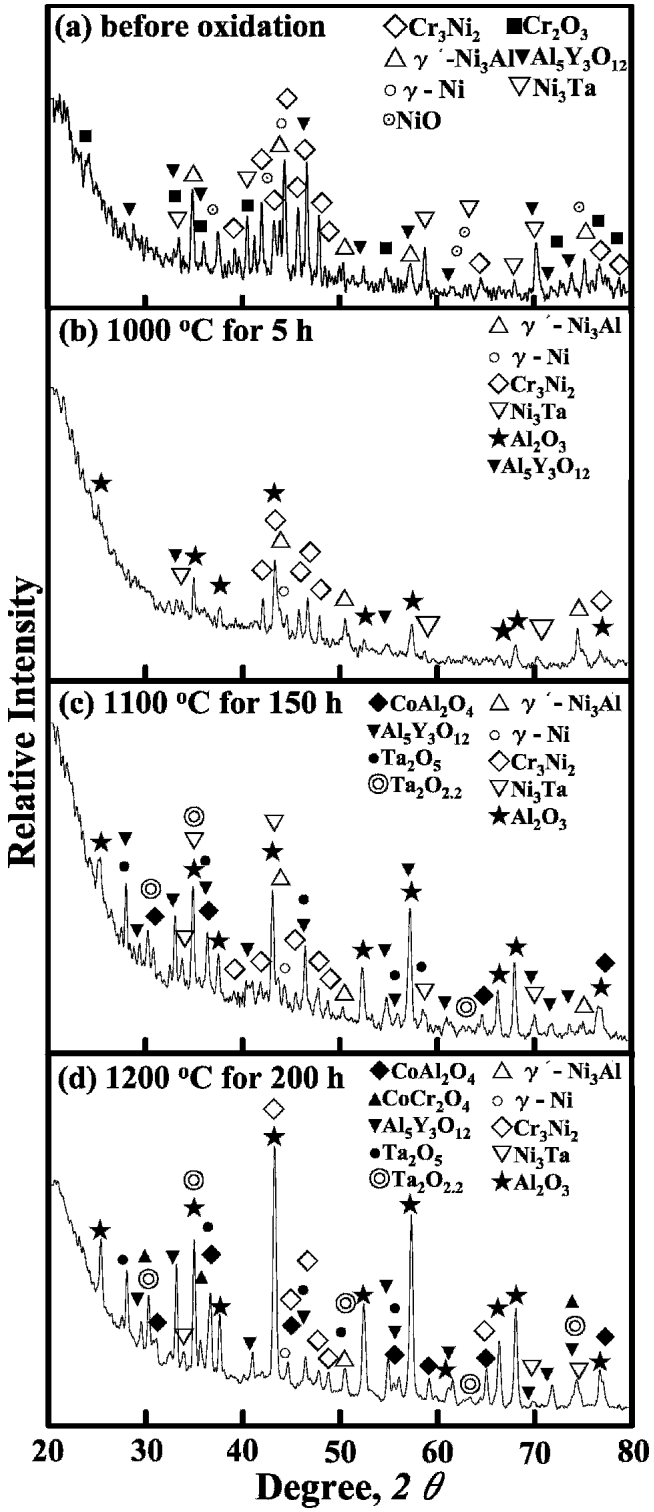

Fig. 2 XRD patterns of HVOF-sprayed Ni-Co-Cr-Al-Y + ReTa coatings before and after oxidation between 1000 and 1200 °C for 5 ~ 200 h in atmospheric air: (a) before oxidation and (b) to (d) after oxidation

Table 2 Phases identified before and after high-temperature oxidation in air, as a function of the spraying method, oxidation conditions, and the powder composition used for spraying

Spraying method	Oxidation temperature/time	Powder composition, wt.%	Before oxidation	After oxidation	Reference
HVOF	1000 ~ 1200 °C/200 h	30Ni-20Co-30Cr-10Al-2Y + 4Re4Ta	Cr_3Ni_2, γ′, Ni_3Ta, γ, NiO, $Al_5Y_3O_{12}$, Cr_2O_3	αAl_2O_3, $Al_5Y_3O_{12}$, $CoAl_2O_4$, $CoCr_2O_4$, Ta_2O_5, $Ta_2O_{2.2}$	This study
HVOF	1000 ~ 1200 °C/200 h	30Ni-30Co-20Cr-12Al-4Y + 4Re	γ′, γ, Cr_3Ni_2, Cr_2O_3	αAl_2O_3, $CoAl_2O_4$, $CoCr_2O_4$, $Al_5Y_3O_{12}$	This study
VPS	950 ~ 1200 °C/260 h	Ni-Co-Cr-12Al-Y + 3Re	γ′, β, γ, σ, α-Al_2O_3	(θ, γ, α)-Al_2O_3, Cr_2O_3	Toma et al. (Ref 5), Brandl et al.(Ref 3)
HVOF	950 ~ 1200 °C/1500 h	Ni-Co-Cr-12Al-Y + 3Re	γ′, β, γ, σ, Y, M_xY_y, α-Al_2O_3, $Al_xY_yO_z$	αAl_2O_3, $NiAl_2O_4$, $CoAl_2O_4$, Cr_2O_3	Toma et al. (Ref 5), Brandl et al. (Ref 3, 4)
LPPS	950 ~ 1000 °C/10,000 h	Ni-Co-Cr-12Al-Y + 3Re, Ni-Co-Cr-24 at.% Al + 3 at.% Re	γ, β, σ, α-Cr	αAl_2O_3, Cr_2O_3, $NiCr_2O_4$, $CoCr_2O_4$, $(Ni,Co)(Al,Cr)_2O_4$, YAl_2O_3	Czech et al. (Ref 7-9)
VPS	950 °C/20,000 h	Ni-Co-Cr-12Al-Y + 3Re	γ, β, σ, α-Cr	αAl_2O_3, Cr_2O_3, Ni-oxides	Beele et al. (Ref 6)
HVOF	1000 ~ 1200 °C/200 h	40Ni-23Co-20Cr-9Al-4Y + 4Ta	γ′, γ, Ni_3Ta, Cr_3Ni_2	αAl_2O_3, $CoAl_2O_4$, $Al_5Y_3O_{12}$, Ta_2O_5, $Ta_2O_{2.2}$	This study
LPPS	850 °C/800 h	Ni-(22-24)Co-(18-21)Cr-(7.5-9.5)Al-(0.7-0.8)Y + (3.5-4.5)Ta	γ′, β, γ, σ, M_5Y	αAl_2O_3, Cr_2O_3	Frances et al. (Ref 11)

Note: β, NiAl; γ, Ni; γ′, Ni_3Al; σ, CrCo; VPS, vacuum plasma spraying

gressed, the scales thickened, resulting in a decrease in the unoxidized coating peaks. Regardless of the oxidation temperature or time, αAl_2O_3 was always the oxide phase that played a major role in protecting the retained coating. The other oxides detected were $Al_5Y_3O_{12}$, $CoAl_2O_4$, $CoCr_2O_4$, Ta_2O_5, and $Ta_2O_{2.2}$.

Table 2 lists the phases that were identified before and after the high-temperature oxidation, as a function of the spraying method, the oxidation conditions, and the powder composition used for spraying. In this study, 30Ni-30Co-20Cr-12A-l4Y + 4Re and 40Ni-23Co-20Cr-9Al-4Y + 4Ta coatings were also prepared for comparison.

In the as-sprayed Ni-Co-Cr-Al-Y + (Re and/or Ta) coatings, Ni was always found. NiAl and Ni_3Al were frequently found and, sometimes, grains of Cr_3Ni_2, σCrCo (Ref 3-9, 11), and αCr (Ref 6-9) were found as well. A very small amount of tiny particles of Y and M_xY_y (Ref 3-5, 11), together with the precipitated oxides of NiO, Cr_2O_3, αAl_2O_3, and $Al_xY_yO_z$ (Ref 3-5) were also found. In particular, Ta formed Ni_3Ta in the Ni-Co-Cr-Al-Y + Ta coatings, whereas Re was never detected in the Ni-Co-Cr-Al-Y + Re coatings, due to its dissolution in other phases, such as αCr and σCrCo (Ref 6-10). Therefore, during spraying, it can be seen that, among the coating elements, Ni is prone to be transformed into Cr_3Ni_2, Ni_3Al, NiAl, NiO, and, if there is any Ta present, into Ni_3Ta. The fact that only σCrCo was found as a cobalt containing phase, despite the high Co content, implies that Co had a tendency to dissolve in the other phases, such as β(Ni,Co)Al (Ref 6) and γ(Ni,Co) (Ref 9). Cr formed Cr_3Ni_2, σCrCo, and Cr_2O_3. Al formed intermetallic compounds of Ni_3Al, NiAl, and a small amount of Al_2O_3 dispersoids (Ref 3-5).

In the oxidized Ni-Co-Cr-Al-Y + (Re and/or Ta) coatings, alumina was always the major oxide. Other oxides formed were Cr_2O_3 (Ref 3-9, 11), $CoAl_2O_4$ (Ref 3-5), $CoCr_2O_4$ (Ref 7-9), $NiAl_2O_4$, and $(Ni,Co)(Al,Cr)_2O_4$ (Ref 3-5, 7-9). Clearly, some Al_2O_3 reacted with CoO and NiO to form more stable spinels. Y existed as $Al_5Y_3O_{12}$ or YAl_2O_3 (Ref 7-9). It is known that Al_2O_3 readily reacts with Y_2O_3 to form $AlYO_3$ (perovskite) and then $Al_5Y_3O_{12}$ (yttria-alumina garnet [YAG]). The presence of YAG increases the oxidation resistance and scale adherence via the pegging effect. A modification to the oxide growth mechanism resulting from the inward diffusion of oxygen ions to the outward diffusion of cations can also be explained as an additional effect of YAG (Ref 12). Especially, Ta was oxidized to Ta_2O_5 and $Ta_2O_{2.2}$, whereas no rhenium oxides were detected. As mentioned above, various inconsistent phases were found both before and after oxidation, depending on the investigator. This may have originated from the nonequilibrium of the rapidly solidified molten droplets during spraying, the different coating composition and the oxidation condition used. It was also noted that the spraying distance, the fuel-to-oxygen ratio, the powder feed rate, and the heat treatment before and after oxidation exert a major influence on the microstructure and oxygen content (Ref 14). Additionally, the nature of the oxidation products depends on the number of defects and pores, which provide easy diffusion paths for ionic movement (Ref 15).

Figure 3 shows the Ellingham diagram of the possible oxides that can be formed on the Ni-Co-Cr-Al-Y + ReTa coating. It can be seen that the oxide stability increases in the order of ReO_2, NiO, CoO, Cr_2O_3, Ta_2O_5, Al_2O_3, and Y_2O_3. The selective oxidation of Al from the surface resulted in the formation of Al_2O_3-rich scales on the Ni-Co-Cr-Al-Y + (Re and/or Ta) coatings. No rhenium oxides were detected in the XRD measurements, due mainly to the dissolution of Re in other oxides. A substantial

amount of Ni was present in the prepared coating. However, no Ni oxides were detected in the XRD measurements obtained of the oxidized specimens examined in this study. Any NiO that formed during spraying and oxidation would react with Al_2O_3 to form the more stable $NiAl_2O_4$ spinel; however, its content was too small to detect using XRD. Because Co is more active than Ni, $CoCr_2O_4$, or $CoAl_2O_4$ are seen in Fig. 2. Also, Ni and Co can be partially dissolved in other oxides. Apparently, the CoO-forming tendency was stronger than the NiO-forming tendency in the present coating. Our XRD results indicated that Cr_2O_3 was absent in the scales, which is inconsistent with the previous results (Ref 3-9, 11). The chromia that formed reacted with CoO to become $CoCr_2O_4$ in this study. It is worthwhile noting that, based on the oxidation of Ni-Co-Cr-Al-Y + Re coating, Czech et al. (Ref 9) reported that Cr_2O_3 and spinels were observed, as well as the major oxide of αAl_2O_3, on the as-sprayed surface in its initial state, whereas a coherent αAl_2O_3 scale with inclusions of $YAlO_3$ formed on the polished surface starting at the beginning of oxidation. The nature of the oxidation products is sometimes dependent on the surface roughness of the coating, because the higher the surface roughness, the more the surface is exposed to the atmosphere. However, it should be noted that Zhao et al. (Ref 15) reported no significant influence of the coating surface roughness on the oxidation behavior. Considering that Cr_2O_3 is completely miscible in Al_2O_3, the coexistence of these two oxides reported in previous studies (Ref 3-9, 11) may have been due to the compositional heterogeneity of the rapidly solidified coating, the nonequilibrium nature of oxidation, or the surface roughness. The most active Y always gave rise to conspicuous $Al_5Y_3O_{12}$ patterns, as explained in Fig. 2, although the initial amount of Y in the coating was small.

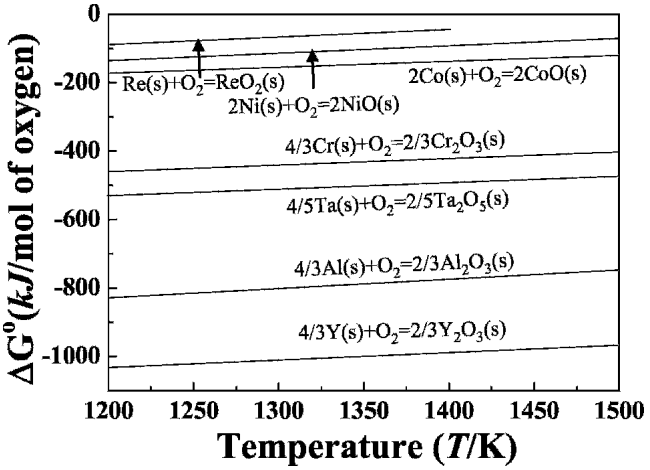

Fig. 3 Ellingham diagram of possible oxides that can be formed on a Ni-Co-Cr-Al-Y + ReTa coating

Figure 4 shows the SEM top view of the Ni-Co-Cr-Al-Y + ReTa coating after oxidation. The size of the oxide particles formed on the surface changed from fine crystallites to coarse grains as the oxidation progressed. The surface of the αAl_2O_3-rich oxide layer was rougher than the original coating surface.

Figure 5 shows the EPMA results of the cross-sectional scales formed on the Ni-Co-Cr-Al-Y + ReTa coating. The Al-rich scales were porous and had cracks owing to the heterogeneous volume expansion that occurred during scaling, which deteriorated the scale adherence. Their thickness was nonuniform, owing to the compositional variation of the sprayed coating. The characteristics of each alloying element in the coating were as follows.

- Aluminum, being the active metal, preferentially oxidizes to Al_2O_3, along with some $Al_5Y_3O_{12}$, $CoAl_2O_4$, and

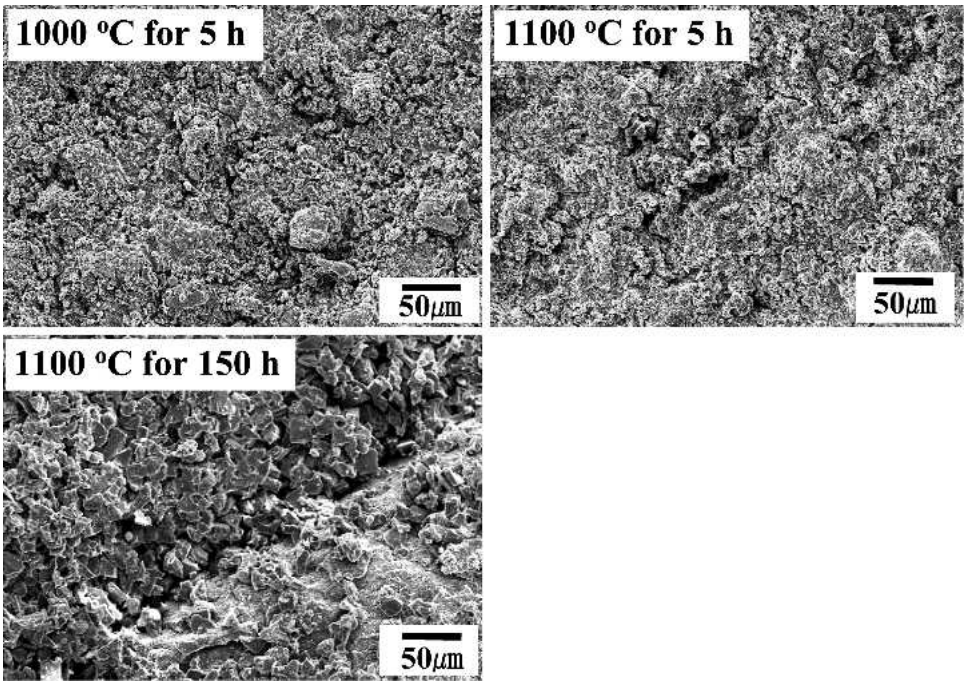

Fig. 4 Top view of an SEM image of a Ni-Co-Cr-Al-Y + ReTa coating after oxidation between 1000 and 1200 °C for 5 ~ 150 h in atmospheric air

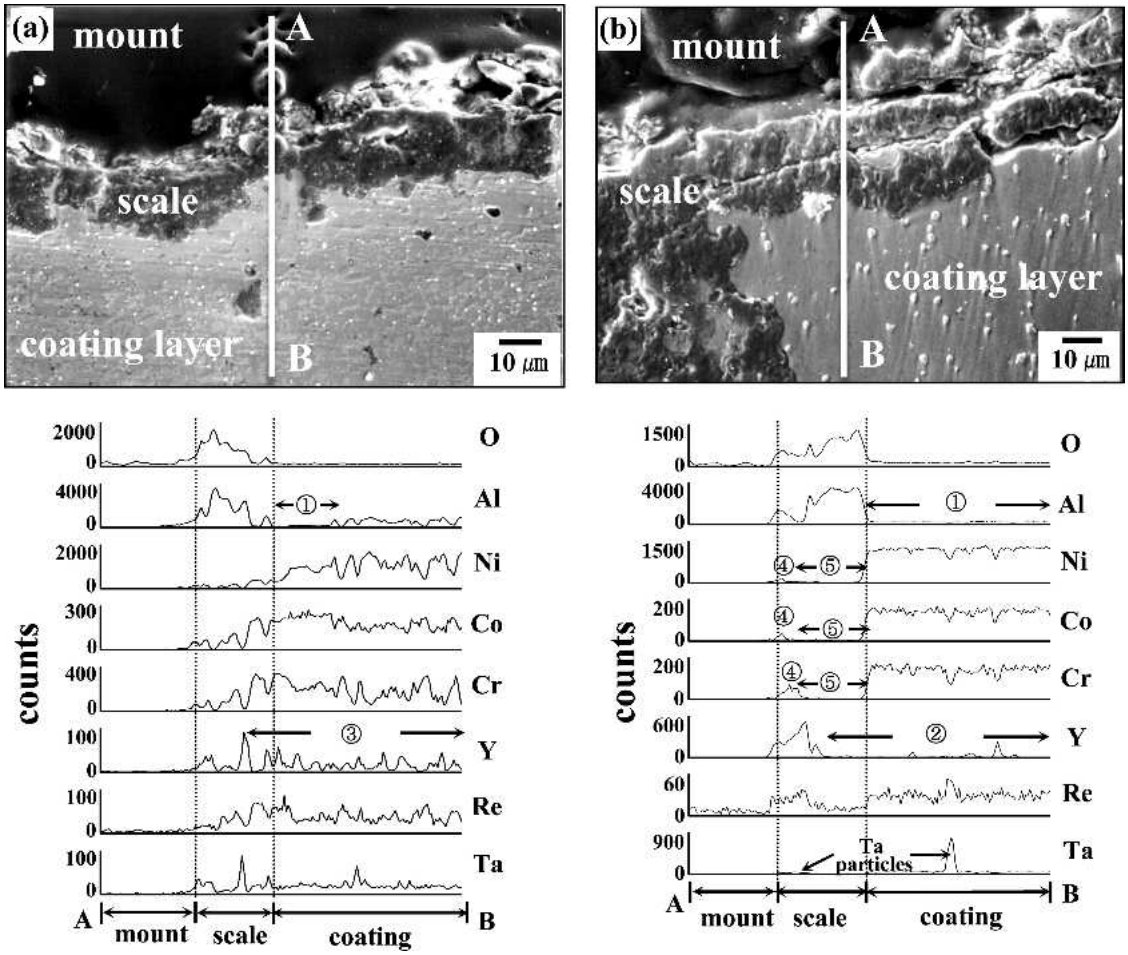

Fig. 5 EPMA results of cross-sectional scales formed on the Ni-Co-Cr-Al-Y + ReTa coating: (a) oxidation at 1000 °C for 200 h; (b) oxidation at 1200 °C for 50 h

$Al_5Y_3O_{12}$. The consumption of Al in the scale leads to the formation of an Al-depleted zone underneath (Ref 16). The more severe the oxidation, the more distinct the Al-depleted zone (see 1 in Fig. 5).

- Yttrium, being the most active metal, oxidizes to $Al_5Y_3O_{12}$, the content of which increases with increasing oxidation temperature and time (Fig. 2). The deficiency of Y (see 2 in Fig. 5) when compared with the corresponding region (see 3 in Fig. 5) may indicate that Y continuously diffuses outward from the coating toward the outer oxide surface until exhaustion. Yttrium is known to increase the oxidation resistance and scale adherence, but some cracking or breakdown of the Al_2O_3-rich scale was still noticed in this study.
- Rhenium, being the most noble metal, is distributed throughout the oxide scale, probably as dissolved ions, and in the unoxidized coating, without forming oxides. No preferential oxidation took place, and no subsequent depletion/enrichment of Re occurred. Based on the high-temperature oxidation of the Ni-Co-Cr-12Al-Y + 3Re coating prepared by the LPPS (Ref 8) and VPS methods (Ref 6), Czech et al. previously reported that Re was not found in the oxide scale but was segregated underneath the oxide scale. The present inconsistent result cannot be due to the addition of Ta, because Re was found in the oxide scale formed on the Ta-free 30Ni-30Co-20Cr-12Al-4Y + 4Re coating prepared for the purpose of comparison. Hence, it is proposed that Re can be incorporated within the oxide, depending on the coating surface roughness (Ref 9), spaying method/parameters, and, more likely, the coating composition.
- Among the different coating elements, Ta can be described as having intermediate oxide stability. It is always oxidized to Ta_2O_5 and $Ta_2O_{2.2}$ in Ni-Co-Cr-Al-Y + Ta(+ Re) coatings. However, these oxides were not found under mild oxidation conditions, but only under severe oxidation conditions (Fig. 2). They were randomly distributed in the scale.
- Ni, Co, and Cr are more noble than Ta (see Fig. 3). They exhibit similar concentration profiles, implying that their activities and diffusivities in the coating are probably similar during oxidation. Upon exposure to oxygen, they were oxidized, constituting a proportion of the outer part of the scale (see 4 in Fig. 5) according to their initial amount. The ensuing consumption of Ni, Co, and Cr at the outer part of the scale thereby resulted in the formation of an (Ni, Co, Cr)-depleted zone underneath (see 5 in Fig. 5). However,

Re and Ta did not form an (Re, Ta)-depleted zone. This difference is attributed to the different consumption rate at the outer part of the oxide scale, the availability and diffusivity of these elements in the oxide scale, as well as to the coating itself.

4. Conclusions

The scales formed on the Ni-Co-Cr-Al-Y + ReTa coating between 1000 and 1200 °C during oxidation in air for up to 200 h consisted mainly of αAl_2O_3, along with some $Al_5Y_3O_{12}$, $CoAl_2O_4$, $CoCr_2O_4$, Ta_2O_5, and $Ta_2O_{2.2}$. αAl_2O_3, which was the major oxidation product, further reacted with the other oxides to a certain extent. The coating elements were generally present at the outer part of the oxide scale, owing to their exposure to high temperature. The ensuing consumption of Ni, Co, Cr, and Y led to the formation of an (Ni, Co, Cr, Y)-depleted zone underneath the outer part of the oxide scale. However, Al was not depleted within the scale, because there was still enough Al that could be supplied to the scale. Rhenium, being the most noble element, was distributed rather uniformly in the scale, without forming any rhenium oxides. However, the more active element, Ta, formed Ta_2O_5 and $Ta_2O_{2.2}$, which were distributed randomly in the scale, due to the low Ta content.

References

1. J.A. Haynes, E.D. Rigney, M.K. Ferber, and W.D. Porter, Oxidation and Degradation of a Plasma-Sprayed Thermal Barrier Coating System, *Surf. Coat. Technol.,* Vol 86-87, 1996, p 102-108
2. J.M. Guilemany, J. Nutting, J.R. Miguel, and Z. Dong, Microstructure Characterization of WC-Ni Coatings Obtained by HVOF Thermal Spraying, *Scripta Metall. Mater.,* Vol 33 (No. 1), 1995, p 55-61
3. W. Brandl, D. Toma, J. Kruger, H. J. Grabke, and G. Matthäus, The Oxidation Behavior of HVOF Thermal-Sprayed MCrAlY Coatings, *Surf. Coat. Technol.,* Vol 94-95, 1997, p 21-26
4. W. Brandl, D. Toma, and H.J. Grabke, The Characteristics of Alumina Scales Formed on HVOF-Sprayed MCrAlY Coatings, *Surf. Coat. Technol.,* Vol 108-109, 1998, p 10-15
5. D. Toma, W. Brandl, and U. Köster, Studies on The Transient Stage of Oxidation of VPS and HVOF Sprayed MCrAlY Coatings, *Surf. Coat. Technol.,* Vol 120-121, 1998, p 8-15
6. W. Beele, N. Czech, W.J. Quadakkers, and W. Stamm, Long-Term Oxidation Tests on a Re-Containing MCrAlY Coating, *Surf. Coat. Technol.,* Vol 94-95, 1997, p 41-45
7. N. Czech, V. Kolarik, W.J. Quadakkers, and W. Stamm, Oxide Layer Phase Structure of MCrAlY Coatings, *Surf. Eng.,* Vol 13 (No. 5), 1997, p 384-388
8. N. Czech, F. Schmitz, and W. Stamm, Microstructural Analysis of the Role of Rhenium in Advanced MCrAlY Coatings, *Surf. Coat. Technol.,* Vol 76-77, 1995, p 28-33
9. N. Czech, M. Juez-Lorenzo, V. Kolarik, and W. Stamm, Influence of the Surface Roughness on the Oxide Scale Formation on MCrAlY Coatings Studied in situ by High Temperature X-ray Diffraction, *Surf. Coat. Technol.,* Vol 108-109, 1998, p 36-42
10. N. Czech, F. Schmitz, and W. Stamm, Improvement of MCrAlY Coatings by Addition of Rhenium, *Surf. Coat. Technol.,* Vol 68-69, 1994, p 17-21
11. M. Frances, M. Vilasi, M. Mansour-Gabr, J. Steinmentz, and P. Steinmentz, Etude de l'Oxydation à 850 °C de l'Alliage Ni-Co-Cr-Al(-Y)-Ta Coulé et Projeté au Chalumeau Plasma sous Pression Réduite, *Mater. Sci. Eng.,* Vol 88, 1987, p 89-96 (in French)
12. H.S. Choi, B.H. Yoon, H.J. Kim, and C.H. Lee, Isothermal Oxidation of Air Plasma Spray NiCrAlY Bond Coatings, *Surf. Coat. Technol.,* Vol 150, 2002, p 297-308.
13. F. J. Belzunce, V. Higuera, and S. Poveda, High Temperature Oxidation of HFPD Thermal-Sprayed MCrAlY Coatings, *Mater. Sci. Eng. A,* Vol 297, 2001, p 162-167
14. E. Lugscheider, C. Herbst, and L. Zhao, Parameter Studies on High-Velocity Oxy-Fuel Spraying of MCrAlY Coatings, *Surf. Coat. Technol.,* Vol 108-109, 1998, p 16-23
15. L. Zhao, M. Parco, and E. Lugscheider, High Velocity Oxy-Fuel Thermal Spraying of a NiCoCrAlY Alloy, *Surf. Coat. Technol.,* Vol 179, 2004, p 272-278
16. L. Ajdelsztajn, J.A. Picas, G.E. Kim, F.L. Bastian, J. Schoenung, and V. Provenzano, Oxidation Behavior of HVOF Sprayed Nanocrystalline NiCrAlY Powder, *Mater. Sci. Eng. A,* Vol 338, 2002, p 33-43